The C-Terminus and Linker Region of S100B Exert Dual Control on Protein−Protein Interactions with TRTK-12[†]

Kimberly A. McClintock,[‡] Linda J. Van Eldik,[§] and Gary S. Shaw*,[‡]

Department of Biochemistry and McLaughlin Macromolecular Structure Facility, The University of Western Ontario, London, Ontario, Canada, N6A 5C1, and Department of Cell and Molecular Biology and Northwestern Drug Discovery Program, Northwestern University Medical School, Ward 4-202, 303 East Chicago Avenue, Chicago, Illinois 60611

Received August 28, 2001; Revised Manuscript Received December 26, 2001

ABSTRACT: S100B, an EF-hand calcium-binding protein composed of two S100β monomers, undergoes a calcium-dependent conformational change that provides a surface for target interactions. In this study, the calcium-sensitive S100B-binding epitope TRTK-12 has been used to probe the contributions of the linker and C-terminal regions of S100B to protein−protein interactions. These contributions were quantified using C-terminal mutant S100B proteins lacking the C-terminal seven (S100B85stop) or nine (S100B83stop) residues or containing alanine substitutions at Phe87 (F87A), Phe88 (F88A), or both (F8788A). Both F8788A and F88A bound TRTK-12 less tightly (K_d = 1.85 ± 0.02 and 0.97 ± 0.08 μM, respectively) than the wild-type protein (K_d = 0.27 ± 0.03 μM, ΔG = −37.2 kJ/mol), indicating these residues are important for TRTK-12 interaction. The truncated S100B proteins bound TRTK-12 much more weakly (K_d = 659.7 ± 119.3 μM, ΔG = −17.9 kJ/mol), indicating the linker region contributed about 50% to the binding of TRTK-12, while the C-terminus contributed the remaining 50% of the binding energy. Based on mutagenesis and NMR chemical shift studies, a comparison with known S100−target protein complexes showed the S100B−TRTK-12 complex has the strongest resemblance to the S100A10−annexin II interaction.

A wide variety of cellular processes such as cell growth and differentiation are controlled by signal transduction pathways that utilize calcium as a second messenger. In many cases, the signaling proteins that control these processes are EF-hand calcium-binding proteins. These proteins react to changes in cellular calcium levels by binding calcium ions, undergoing a conformational change, and interacting with target proteins. Two notable members of this family include the ubiquitous protein calmodulin and the muscle protein troponin-C. Three-dimensional structures of these proteins in their apo forms (*1*−*4*) and calcium-bound forms (*1*, *2*, *5*−*10*) have revealed the details of their calcium-induced conformational changes. In general, calcium binding induces a change in orientation of helices resulting in the exposure of a hydrophobic surface for target protein interactions. Recently, several three-dimensional structures from the S100 calcium-binding protein family have indicated these proteins may operate using a similar mechanism (*11*−*17*). S100s have been found to interact with a diverse group of proteins in a calcium-sensitive manner including those involved in cellular architecture, cell cycle regulation, and neurite outgrowth [for review, see (*18*)].

S100B is one of the best-studied members of the S100 family. The protein is a 21 kDa dimer composed of two 91-residue S100β subunits. Each subunit contains 2 calcium-binding sites; site I, a pseudo-EF-hand comprised of helices I and II and a 14-residue calcium-binding loop; and site II, a canonical EF-hand comprised of helices III and IV and a 12-residue loop. The three-dimensional structures of apo-S100B and calcium-bound S100B have shown that calcium binding leads to a significant conformational change in site II resulting in a reorientation of helix III and lengthening of helix IV (*15*, *19*). This structural change exposes previously buried hydrophobic residues in the C-terminus and the linker region of S100B, forming a possible recognition surface for calcium-dependent protein−protein interactions (*15*). Similar to the target recognition site in calmodulin, this surface on S100B appears to be composed primarily of acidic and hydrophobic residues. Further, S100B displays a calmodulin-like promiscuity, interacting with more than 20 potential target proteins in a calcium-dependent manner [for review, see (*18*)]. For example, S100B has been shown to inhibit the phosphorylation of several proteins including tau (*20*, *21*), MARCKS (*22*), and neuromodulin (GAP-43) (*23*). Additionally, through calcium-dependent interactions with tubulin, desmin, and glial fibrillary acidic protein (GFAP),[1]

[†] This research was supported by operating and maintenance grants from the Canadian Institute for Health Research (G.S.S.) and graduate studentships to K.A.M. from the Alzheimer Society of London and Middlesex and the Natural Sciences and Engineering Research Council. Funding for the NMR spectrometer in the McLaughlin Macromolecular Structure Facility was made possible through grants from the Medical Research Council of Canada and the Academic Development Fund of The University of Western Ontario and generous gifts from R. Samuel McLaughlin Foundation and London Life Insurance Co. of Canada. This research was also supported in part by NIH Grant AG13939 (L.J.V.E.).

* To whom correspondence should be addressed. Phone: 519-661-4021. Fax: 519-661-3175. Email: shaw@serena.biochem.uwo.ca.

[‡] The University of Western Ontario.

[§] Northwestern University Medical School.

10.1021/bi011732m CCC: $22.00
Published on Web 03/30/2002

S100B can inhibit the assembly of these cytoskeletal molecules (*24*−*27*).

An S100B-binding sequence was identified using a random bacteriophage library (*28*). This study and others have shown that peptides containing the consensus sequence (R/K)(L/I)(XWXXIL) bind to S100B in a calcium-sensitive manner. Further, sequence analysis reveals the presence of the consensus sequence in conserved regions in several cytoskeletal proteins previously shown to interact with Ca^{2+}-S100B including GFAP, desmin, vimentin, and tubulin (*29*). A synthetic peptide derived from this sequence (TRTK-12) has since been shown to compete for Ca^{2+}-S100B binding with other proteins such as CapZ-α and GFAP (*27*, *28*). In addition, the TRTK-12 interaction with S100B is calcium-dependent and of similar affinity (1 μM)(*30*) to other calcium-binding protein−peptide interactions (*30*−*32*).

A three-dimensional structure of the calcium-bound S100B dimer in complex with the TRTK-12 peptide is not yet available. However, some information can be gleaned from other three-dimensional structures of S100 proteins complexed with target peptides (*33*−*35*). The structure of Ca^{2+}-S100B in complex with a 23-residue peptide derived from the negative regulatory domain of p53 shows several contacts between the p53 peptide and the central part of the C-terminus and helix III within a single S100*β* monomer (*35*). This mode of interaction is significantly different from that of the S100A10−annexin II and S100A11−annexin I complexes, where the peptide interacts primarily with the C-terminus and the linker regions of one S100 monomer and extends to helix I of the second S100 monomer, thus bridging the dimeric S100 structure (*33*, *34*). The structures of these S100 complexes suggest that different modes of interaction may exist for different S100 proteins with different targets. In the current work, we present the first site-directed mutagenesis studies of human S100B aimed at identifying key regions and residues required for the interaction with TRTK-12. We have used these studies to provide the first quantitative picture of the relative importance of these regions for target protein interaction and to establish whether the S100B−TRTK-12 interaction is similar to either the annexin interactions with S100A10/S100A11 or the p53−S100B interaction.

EXPERIMENTAL PROCEDURES

Materials. Calcium chloride was puratronic grade from Alfa-Aesar (Mississauga, Canada). All other chemicals were of the highest purity commercially available. The TRTK-12 peptide (Ac-TRTKIDWNKILS-NH_2) was synthesized by the Queen's Peptide Synthesis Lab (Queen's University, Kingston, Canada). Purity was confirmed using reversed-phase HPLC and mass spectrometry. Deuterated PIPES buffer (d_{16}, 99%+; OD, 70%) was obtained from Cambridge Isotope Laboratories (Andover, MA).

Recombinant human (wild-type, F87A, F88A, F8788A) and bovine (S100B83stop, S100B85stop) S100B proteins were expressed in *E. coli* (strain N99) and purified as previously described (*36*). Uniformly labeled S100B85stop protein was ^{15}N-labeled and purified as described previously for wild-type S100B (*19*). The F88A mutant contains Phe (TTT) to Ala (GCC) mutations at positions 329−331 of the human S100B expression vector pSS2. The construction of this vector has previously been described (*36*). The F87A mutant contains a Phe (TTC) to Ala (GCC) mutation at positions 326−328 of pSS2, and F8788A has both mutations. The bovine S100B mutants S100B83stop and S100B85stop were constructed and expressed in the pVUSB-1 vector (*37*). In the truncation mutants S100B85stop and S100B83stop, residues His85 and Ala83, respectively, have been changed to stop codons (TAA), resulting in mutant proteins lacking the C-terminal seven and nine residues, respectively.

Fluorescence Spectrophotometry. Standard fluorescence experiments were conducted using solutions of TRTK-12 peptide in buffer containing 50 mM Tris, 50 mM KCl, and 1 mM $CaCl_2$ at pH 7.2. Experiments involving changes in pH utilized KCl concentrations of 50 mM at pH 5.6, 6.2, and 8.5 while those probing ionic strength used KCl concentrations of 5, 50, and 150 mM at pH 7.2. The TRTK-12 concentration in 50 mM Tris (pH 7.2) and 50 mM KCl was determined from absorbance spectra using an extinction coefficient of $\epsilon_{280} = 5600\ cm^{-1}\ M^{-1}$. Concentrations of S100B stock solutions were determined using the Bio-Rad protein assay performed in triplicate and a standard curve of S100B based on amino acid analysis (Alberta Peptide Institute, Edmonton, Canada).

Titrations of TRTK-12 with Ca^{2+}-S100B were carried out at ambient temperature using a stirred cell holder. S100B proteins were added in 1−3 μL aliquots using a calibrated 10 μL Hamilton syringe. Total sample volumes did not change by more than 3%. Following each S100B addition, the samples were allowed to equilibrate for 1 min with stirring before scanning. Titrations were carried out to a final S100*β*:peptide ratio of 4:1. Emission spectra were obtained using a fluorescence spectrophotometer model RF-M2004 (Photon Technology International) using an excitation wavelength of 295 nm. Fluorescence emission was recorded from 305 to 400 nm using an emission band-pass of 2 nm. An increase in fluorescence intensity at 333 nm was used to monitor the interaction of TRTK-12 with the S100B protein.

Chemical Cross-Linking. S100B or S100B85stop (16 μM) was incubated at ambient temperature for 20 min in 50 mM HEPES, 150 mM NaCl (pH 7.5) plus or minus TRTK-12 (12, 32, or 80 μM). Samples contained either 1 mM $CaCl_2$ or 1 mM EDTA (final reaction volume 50 μL). Following this, a 20-fold excess of the 11.4 Å cross-linker bis(sulfosuccinimidyl) suberate (BS^3) (0.5 μL) in 5 mM sodium citrate buffer (pH 5.0) was added. After a 30 min incubation, the reactions were quenched for 15 min with an excess of ethanolamine and analyzed by SDS−PAGE (15% Tricine).

NMR Spectroscopy. Proteins were dissolved in 90% H_2O/10% D_2O, 5 mM DTT, 4 mM $CaCl_2$, pH 7.0. NMR spectra were acquired at 35 °C on a Varian Unity 500 MHz spectrometer equipped with a triple-resonance, pulsed-field gradient probe. Carrier frequencies used were centered at 120.00 (^{15}N) and 4.73 (^1H) ppm. Two-dimensional ^1H-^{15}N HSQC experiments were acquired on 200 μM ^{15}N-S100B85stop samples using the sensitivity-enhanced method (*38*) as described previously (*19*). The dissociation constant for the binding of ^{15}N-S100B85stop to TRTK-12 was determined by plotting the changes in chemical shift of I47,

[1] Abbreviations: HSQC, heteronuclear single quantum correlation; GFAP, glial fibrillary acidic protein; Ca^{2+}-S100B, calcium-bound S100B; DTT, dithiothreitol; PIPES, piperazine-*N*,*N*′-bis(2-ethanesulfonic acid); BS^3, bis(sulfosuccinimidyl) suberate.

V52, and V53 upon each TRTK-12 addition based on the formula: $\Delta\delta|(^1H)| + 0.2*\Delta\delta|(^{15}N)|$ (*39*).

pK_a values for His 85 and His 90 were determined using one-dimensional ^1H experiments. S100B was exchanged by dissolving the protein in D_2O at pH 8.0 and incubating for 72 h. The TRTK-12 peptide was allowed to exchange for 16 h after being dissolved in D_2O. The spectra were recorded with a spectral window of 6000 Hz, an acquisition time of 2 s, and 512 transients per spectrum. The sample contained 0.5 mM S100β, 2 mM $CaCl_2$, 0.8 mM TRTK-12, and 30 mM PIPES buffer. The pH of the sample was adjusted during the titration by adding microliter aliquots of 1% DCl and was measured at room temperature using a calomel electrode (Aldrich).

Dissociation constants and pK_a values were determined using the program Xcrvfit (University of Alberta). Fluorescence and NMR titration data were fit using a 1:1 ratio of TRTK-12 to S100β monomer as described previously (*40*). Attempts to fit the data for different TRTK:S100B stoichiometries resulted in only very slight differences in the dissociation constant and did not change the relative binding affinities of the proteins. Some fits exhibited an initial increase in fluorescence below the 1:1 ratio, believed to result from nonspecific binding of TRTK-12 by S100B at extremely high peptide:monomer ratios in this region of the curve.

RESULTS

S100B has been shown to bind to more than 20 potential targets in a calcium-sensitive manner. Recently, a structure of rat S100B in complex with a peptide from the tumor suppressor protein p53 indicated that the central portion of the C-terminal helix and helix III form the binding site for p53 (*35*). Three-dimensional structures of both S100A10 and S100A11 in complex with target molecules (*33*, *34*) describe an alternate binding surface encompassing the linker region and C-terminus of helix IV. These studies indicate that subtle differences between the target protein sequence and that of the S100 protein are likely responsible for both recognition and the magnitude of the interaction. In this work, we have quantified the contributions to target peptide binding by S100B in order to identify potential residues that control the recognition of the TRTK-12 binding sequence and establish whether the S100B−TRTK-12 interaction bears any resemblance to either of the previously characterized S100−target protein complexes.

A series of mutations were made using human and bovine S100B proteins. Typical of the high conservation between S100B sequences, these proteins are 96.7% identical, with all differences being conservative substitutions. At positions 7 and 80, valine and isoleucine in bovine S100B replace methionine and valine residues, respectively, in human S100B. The only other difference is at position 62 where an asparagine in the human protein is replaced by a serine in bovine S100B. These substitutions have little or no impact on the three-dimensional structure of the S100B protein. The regions and residues targeted for protein interaction studies are shown in Figure 1. The proteins include those truncated at the C-terminus (S100β85stop, S100β83stop) and having specific substitutions in this region (F87A, F88A, and F8788A). These mutants were designed based on observations that the C-terminal helix in human S100B has one extra

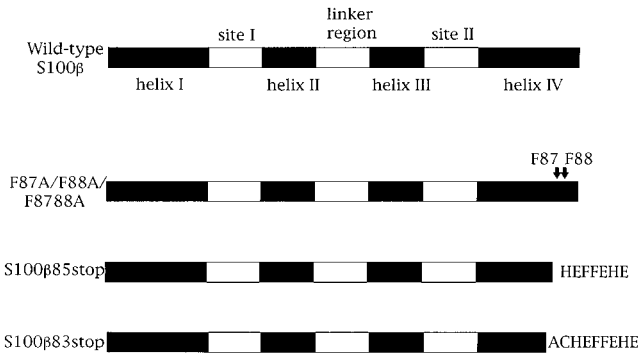

FIGURE 1: Schematic of wild-type and mutant S100β proteins. The two calcium-binding sites (site I and site II) as well as helices I−IV and the linker region between the two EF-hands are indicated for the wild-type monomer. Phenylalanine 87, 88, or both are replaced by alanine in F87A, F88A, and F8788A, respectively. S100β85stop and S100β83stop are C-terminal truncation mutants lacking the last seven and nine residues, respectively, and indicate the monomeric forms of the proteins while S100B85stop and S100B83stop denote the dimeric proteins.

helical turn, including residues F87 and F88, in the calcium form compared to the apo-protein. Further, the C-terminus in the S100 proteins is one of the most highly divergent regions, having little similarity between S100 protein sequences. This region is also absent in the S100 protein member calbindin D_{9k} which does not interact with any known protein or sequence in a calcium-dependent manner.

Importance of the C-Terminal Region of S100B for Interaction with TRTK-12. TRTK-12 binding to S100B was monitored as previously described using the intrinsic fluorescence of the single Trp residue in TRTK-12 (*30*). Since S100B contains no Trp residues, this was a convenient method for measuring interactions between the peptide and the protein. The fluorescence spectrum of TRTK-12 in the absence of Ca^{2+}-S100B exhibited an emission maximum at 348 nm, consistent with a polar, aqueous environment for the tryptophan residue (Figure 2A). Upon addition of Ca^{2+}-S100B, the emission intensity increased and exhibited a blue shift to 333 nm indicating movement of the Trp residue to a more hydrophobic environment from binding to Ca^{2+}-S100B. Consistent with this, significant changes were observed in ^1H-^{15}N HSQC and ^1H NMR experiments as previously reported (*30*). The titration curve for the TRTK-12/Ca^{2+}-S100B interaction (Figure 2B) indicated a 1:1 TRTK-12/S100β monomer stoichiometry and a K_d of 0.27 $\pm$ 0.03 μM. This corresponds to a free energy of binding ($\Delta G_{binding}$) of −37.2 kJ/mol for the interaction of TRTK-12 with calcium-bound S100B (Table 1). This K_d is slightly lower than found in our earlier studies and can be attributed to N- and C-terminal modifications (acetylation and amidation, respectively) of the peptide used in the current study. These modifications result in the neutralization of charge at the peptide termini and would likely stabilize an α-helical conformation (*41*), the structure of TRTK-12 in the bound state (unpublished results).

The C-terminal truncation mutants S100B85stop and S100B83stop were designed to probe the requirement of residues in the C-terminus for TRTK-12 binding. These mutants lacked the C-terminal seven (HEFFEHE) and nine (ACHEFFEHE) residues, respectively, including some residues (F87, F88) suggested as critical for maintenance of the dimeric structure of S100B (*12*, *13*). Sedimentation equilib-

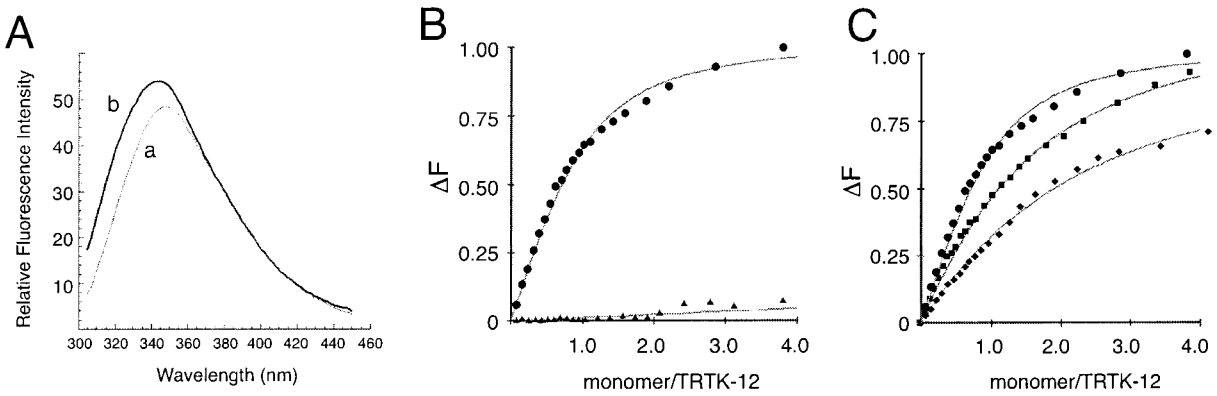

FIGURE 2: Trytophan fluorescence of the TRTK-12 peptide. Samples were prepared in standard buffer (50 mM Tris, 50 mM KCl, 1 mM $CaCl_2$, pH 7.2). (A) Fluorescence of W7 of TRTK-12 (1.05 μM) in the absence (a) and presence (b) of 1 μM S100β. In the absence of S100B, TRTK-12 has an emission maximum at 348 nm, consistent with the tryptophan residue in a polar, aqueous environment. Upon addition of S100B, an increase in fluorescence intensity occurs, and the emission maximum undergoes a blue shift to 333 nm, indicating the movement of the Trp residue to a less polar environment. (B) Titration of TRTK-12 with wild-type S100B (●) and the C-terminal truncation mutant S100B85stop (▲). Tryptophan fluorescence of TRTK-12 was measured at 333 nm, and the change in fluorescence (ΔF) is shown as a function of monomer:TRTK-12 ratio for 1.05 μM TRTK-12. The dissociation constant for TRTK-12 interaction with wild-type S100B was determined to be 0.27 ± 0.03 μM. Curve-fitting for the S100B85stop protein yielded a K_d >1000 μM. A similar result was obtained for S100B83stop (data not shown). The wild-type curve is also presented in (C) for comparison purposes. (C) Titration of TRTK-12 with F88A and F8788A proteins. The dissociation constants for the interaction of F88A (■) and F8788A (◆)with TRTK-12 were 0.97 ± 0.08 and 1.85 ± 0.02 μM, respectively.

Table 1: Dissociation Constants for S100B Proteins and TRTK-12 in 50 mM Tris, 50 mM KCl (pH 7.2)

S100B protein	K_d (μM)	$\Delta G_{binding}$[a] (kJ/mol)
wild-type	0.27 ± 0.03	−37.2
F87A	0.09 ± 0.02	−39.9
F88A	0.97 ± 0.08	−34.1
F8788A	1.85 ± 0.02	−32.5
S100B85stop	659.7 ± 119.3	−17.9

[a] $\Delta G_{binding} = RT \ln K_d$.

rium studies at concentrations similar to those used for the current fluorescence work (1−10 μM) indicated S100B85stop (molecular mass calculated, 19.4 Da; molecular mass observed, 19.0 ± 0.05 Da) and S100B83stop (molecular mass calculated, 19.1 Da; molecular mass observed, 18.5 ± 1.2 Da) remained in a folded, dimeric state in solution. Further, both of these proteins retain their ability to bind calcium (not shown). Interactions of TRTK-12 with the calcium-bound forms of S100B85stop (Figure 2B) and S100B83stop (not shown) were studied by fluorescence spectrophotometry in the same manner as wild-type S100B. Upon addition of these proteins to TRTK-12, the characteristic blue shift seen in the presence of wild-type S100B was not observed and the emission maximum remained essentially unchanged at 348 nm even in the presence of a 4-fold monomer excess of the mutant proteins. Using these data, the estimated K_d for these proteins toward the TRTK-12 peptide appeared to be greater than 1 mM.

Since the measurement of binding used here relied on interaction of the single tryptophan residue in TRTK-12 (W7) with Ca^{2+}-S100B, the possibility existed that the peptide was interacting with the truncated S100B proteins and was undetectable by this method. Such an effect would be expected if W7 remained in a polar, aqueous environment and did not become buried upon binding. To determine whether binding to S100B85stop was occurring but was not detectable by the fluorescence method, we monitored the titration of calcium-bound ^{15}N-labeled S100B85stop protein with TRTK-12 by NMR spectroscopy. The ^{1}H-^{15}N HSQC spectra obtained for S100B85stop were very similar to those for the full-length protein with the notable absence of residues such as F87, F88, and E91 (Figure 3A, light contours). Upon addition of TRTK-12, several residues experienced substantial changes in chemical shift (Figure 3A, dark contours). Notably, several of these were for residues in the linker region (S41, H42, I47) and the adjacent N-terminus of helix III (V52, V53). Further, the observed chemical shift changes were very similar to those seen for the full-length protein. These observations indicated that an interaction between TRTK-12 and S100B85stop occurred even in the absence of the C-terminus of S100B. Based on the normalized average change in chemical shift for I47, V52, and V53, a K_d = 659.7 μM, corresponding to $\Delta G_{binding}$ = −17.9 kJ/mol, was determined (Table 1). This value for $\Delta G_{binding}$ represented about 48% of that for TRTK-12 binding to full-length S100B.

To more clearly define the TRTK-12 interacting regions in S100B85stop and compare these to wild-type S100B, normalized chemical shift changes resulting from TRTK-12 binding to each of these proteins were plotted (Figure 3B). Changes in chemical shift were measured for 39 of 81 possible common residues in S100B85stop that had clearly resolved peaks in both the calcium-bound and peptide-bound spectra. The graph shows three distinct regions where the largest changes in chemical shift are clustered for both the wild-type and mutant proteins. These included residues D12 and S18 in the N-terminus; S41, H42, and I47 in the linker; V52, V53, V56, and V59 in helix III; and F73 and A83 in helix IV. In wild-type S100B, significant changes in chemical shift are also noted for residues 87, 88, and 90 at the extreme C-terminus which are absent in the S100B85stop protein. However, the very strong similarities in chemical shift changes in the linker regions for these proteins indicate that this region is important for the TRTK-12−peptide interaction.

To further confirm an interaction between the S100B85stop protein and the TRTK-12 mutant protein, we performed chemical cross-linking experiments using the cross-linker BS^3. This cross-linker prefers cross-linking of two side chain

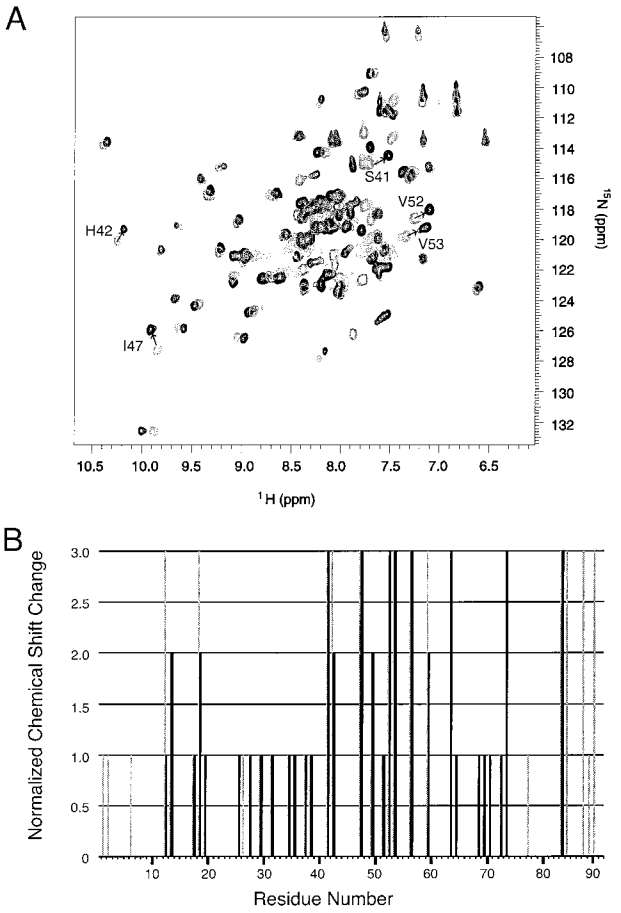

FIGURE 3: Effect of TRTK-12 binding to S100B85stop. (A) ^{1}H-^{15}N HSQC spectrum of uniformly ^{15}N-labeled S10085stop. ^{15}N-labeled Ca^{2+}-S100β85stop (200 μM) is shown in the absence (light contours) and presence (dark contours) of an excess of TRTK-12 (1200 μM) in 90% H_2O/10% D_2O, pH 7.10. The arrows indicate the change in resonance position of residues S41, H42, I47, V52, and V53 in S100β85stop upon addition of TRTK-12. The dissociation constant for the interaction of TRTK-12 and S100β85stop (659.7 $\pm$ 119.3 μM) was determined by plotting the average change in chemical shift for these residues against the ratio of TRTK-12/S100β85stop at each point in the titration. (B) Chemical shift changes in wild-type S100B (gray bars) and S100B85stop (black bars) resulting from TRTK-12 binding. Normalized chemical shift changes were calculated as described under Experimental Procedures for residues in S100B and S100B85stop. For simplicity, the normalized values were grouped into four broad ranges ($0 < \Delta\delta \leq 0.05$ ppm, $0.05 < \Delta\delta \leq 0.15$ ppm, $0.16 < \Delta\delta \leq 0.25$ ppm, and $\Delta\delta > 0.25$ ppm) and assigned relative shift values of 0 ($\Delta\delta \leq 0.05$ ppm, smallest effect), 1, 2, and 3 ($\Delta\delta > 0.25$ ppm, largest effect). Residues 85−91 in S100B85stop and residues that could not be assigned due to overlap were assigned values of 0.

amine groups within a cross-linker reach of 11.4 Å. Cross-linking of TRTK-12 in the presence of $CaCl_2$ with either wild-type S100B or S100B85stop protein yielded a cross-linked product with high efficiency in a concentration-dependent manner (Figure 4). Upon addition of EDTA, the efficiency of cross-linking was significantly reduced (lane 9). The cross-linked product ran slightly slower than the monomeric S100B protein on SDS−PAGE gels, consistent with a cross-link between TRTK-12 and each S100β protein. Cross-linking with shorter-reach cross-linking agents such as sulfo-DST (6.4 Å) and EDC/sulfo-NHS (zero-length) failed to produce any observable product. S100B contains seven lysine residues (K5, K24, K26, K28, K29, K33, K48, K55) while TRTK-12 contains two (K4, K9). The observation that cross-linking was observed with S100B85stop indicates that either K4 or K9 in TRTK-12 lies within 11.4 Å of the lysine residues in the protein. Since the change in chemical shift analysis indicates that residues in the linker of S100B and S100B85stop are more affected by TRTK-12 binding, the most likely candidates for interaction are K48 and K55.

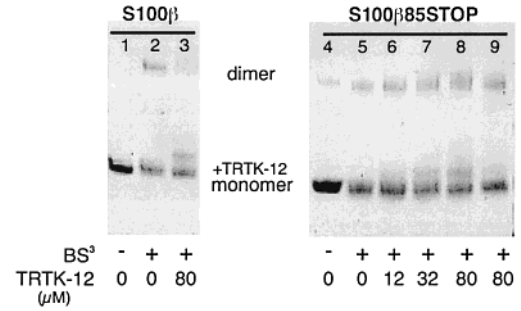

FIGURE 4: Cross-linking of S100B proteins to TRTK-12. S100B (lanes 1−3) or S100B85stop (lanes 4−9) was prepared as described under Experimental Procedures. Briefly, S100 proteins (16 μM) were incubated with varying concentrations of TRTK-12 (0−80 μM) in the presence of 1 mM $CaCl_2$ (lanes 1−8) or 1 mM EDTA (lane 9) prior to addition of an excess of the cross-linker BS^3. Lanes 1, 2, 4, and 5, S100 protein alone; lanes 3, 6, 7, 8, and 9, in the presence of TRTK-12. The presence or absence of cross-linker and the TRTK-12 concentration in each sample are indicated below the figure. Approximate positions of monomeric and dimeric species are indicated. The band shift resulting from cross-linking to TRTK-12 is shown for the monomeric species (+TRTK-12).

Structure of the A83−H85 Region in the S100B−TRTK-12 Complex. In all three-dimensional structures of S100 proteins to date, the central region of helix IV, comprising residues A83−H85, is α-helical (*11*−*17*). In Ca^{2+}-S100B, this results in a partial exposure (104−130 Å^2) of the side chains of these residues. The helix extends to F88 in Ca^{2+}-S100B where the protein then adopts a more random structure (*16*, *19*). The possibility existed that the truncated protein S100B85stop might adopt a similar helical configuration having the extreme C-terminus of its helix IV (i.e., T82, A83, C84) unstructured. In this state, the environment of residues T82−C84 would be perturbed compared to the full-length protein, and binding to TRTK-12 could be significantly affected.

The backbone structures of S100B and S100B85stop in the presence of both calcium and TRTK-12 peptide were assessed using ^{15}N NOESY-HSQC experiments. One particularly diagnostic resonance was that of A83 NH because it is well resolved in both complexes and correlations typical of α-helical structure are easily visible. Figure 5 shows the nOe correlations for A83 NH are markedly different for the S100B and S100B85stop complex. In the S100B−TRTK-12 complex, backbone nOes were observed from A83NH to V80αCH and T82NH. These are indicative of α-helical structure in this region of the protein. In contrast, A83NH in the S100B85stop−TRTK-12 complex exhibited only a weak intraresidue correlation to its βCH_3 group and no interresidue correlations. This indicates that the C-terminus of S100B85stop in the TRTK-12 complex is not α-helical and is likely highly unstructured.

Contribution of F87 and F88 to the TRTK-12 Interaction. Two prime candidates for the interaction of TRTK-12 with the C-terminus of S100B are F87 and F88. These hydro-

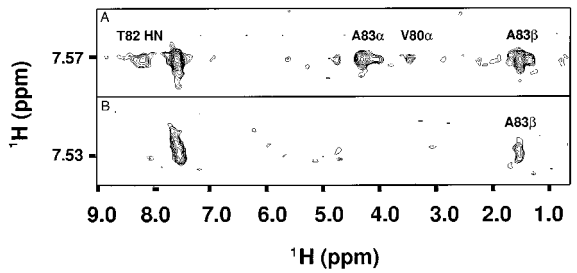

FIGURE 5: Strip plots of A83 extracted from ^{15}N-edited NOESY−HSQC spectra (τ_m = 150 ms) of S100B proteins in complex with TRTK-12. (A) shows correlations to A83 in the wild-type S100B−TRTK-12 complex. Strong intraresidue correlations to A83 Hα and βCH_3 are visible. Interresidue correlations to V80 Hα and T82 HN indicate α-helical structure in this region of the protein. Weak or absent intraresidue correlations in the S100B85stop−TRTK-12 spectrum (B) as well as the lack of the characteristic $d_{\alpha N}(i,i+3)$ nOe correlation indicate a lack of structure at the C-terminus of the mutant protein.

phobic residues increase in surface exposure upon calcium binding. The proteins F87A, F88A, and F8788A were constructed to reduce the hydrophobicity of the side chains at positions 87 and 88 while maintaining the propensity for α-helix formation since this secondary structure is found in this region of Ca^{2+}-S100B (*15*). Unlike the truncation mutants, the fluorescence emission maximum for TRTK-12 exhibited the characteristic blue shift in the presence of all three mutants, indicating interaction of the peptide with these proteins. An interesting finding was observed for the F87A protein, where titration of TRTK-12 with F87A resulted in a larger maximum fluorescence intensity for TRTK-12 compared to wild-type S100B (data not shown). This resulted in an increased affinity (K_d = 0.09 μM) between TRTK-12 and the F87A mutant compared to wild type (Table 1). Further, during the course of this experiment, it was clear that a weaker interaction was occurring with both F88A and F8788A S100B proteins. Figure 2C shows some of the results for the titration of TRTK-12 with each protein. The graph shows that F88A had an affinity about 4 times weaker (K_d = 0.97 μM) and F8788A bound about 7 times weaker (K_d = 1.85 μM) than S100B. These results indicate that residues F87 and F88 play important roles in the S100B/TRTK-12 interaction.

Ionic Nature of the S100B/TRTK-12 Interaction. The C-terminal seven residues of S100B consist largely of acidic and hydrophobic residues (HEFFEHE). At neutral pH similar to that used in this work (pH 7.2), H85 and H90 are the only C-terminal residues that are ionizable, with their imidazole side chains having pK_as of 6.70 ± 0.05 and 7.13 ± 0.04, respectively, as determined by proton NMR titration experiments (data not shown). To determine whether the ionic states of H85 and H90 are important for the interaction with TRTK-12, the binding of the peptide by Ca^{2+}-S100B was also studied at pH 6.2 and pH 8.5 where the histidine residues would be expected to be mostly protonated or deprotonated, respectively. At pH 6.2, the protein had a slightly higher affinity for TRTK-12 (K_d = 0.17 ± 0.03 μM). Upon further decrease of the pH to 5.6, the affinity was close to that at pH 7.2. The dissociation constant at pH 8.5 (K_d = 0.25 ± 0.03 μM) was very similar to those at the other pH values studied. Based on these data, the degree of protonation of H85 and H90 did not appear to affect the binding of TRTK-12 by Ca^{2+}-S100B.

The C-terminal region of S100B also contains three glutamate residues (E86, E89, E91), and since the TRTK-12 peptide contains basic residues at several positions (R2, K4, K9), it might be expected that ionic interactions between these residues and the acidic glutamate residues could have a significant impact on the TRTK-12/S100B interaction. We used increasing ionic strength to probe this interaction using KCl concentrations of 5 and 150 mM in addition to 50 mM used for most experiments. At higher ionic strengths, hydrophobic interactions become more important as electrostatic interactions are screened out. Typically, this results in a decreased binding affinity if ionic binding interactions are important and tighter binding if the interaction is primarily hydrophobic. Interaction of TRTK-12 with Ca^{2+}-S100B under low salt conditions (5 mM) yielded a dissociation constant of 0.20 ± 0.02 μM, similar to that obtained using 50 mM KCl. Under higher salt conditions (150 mM KCl), the titration data were more difficult to interpret due to a more pronounced initial increase in fluorescence (possibly due to nonspecific binding at very high TRTK-12:S100B ratios). Nonetheless, a significantly decreased dissociation constant was observed for TRTK-12 with S100B at high salt concentrations (0.08 ± 0.01 μM). A tighter interaction between S100B and TRTK-12 at higher salt concentrations was supported by NMR titration experiments. At low KCl concentrations, binding of TRTK-12 to S100B occurred in the fast exchange limit. At 150 mM KCl, binding of TRTK-12 to Ca^{2+}-S100B shifts to the slow exchange limit. These observations would be expected from a decreased k_{off} for peptide binding at 150 mM and would be reflected in a decreased K_d. These data likely indicate that ionic interactions play a minor role in the TRTK-12 interaction with S100B and the primary interactions are hydrophobic in nature.

DISCUSSION

The aim of the present study was to identify important residues and quantify their respective contributions to the S100B−TRTK-12 interaction. Three-dimensional structures of three S100 proteins in complex with unique target proteins have recently shown that different portions of the C-terminus and either helix III or the linker regions are responsible for target interactions (*33*−*35*). These observations suggest that differences between the individual S100 sequences and the target protein sequences must provide unique recognition sites for binding and that it is not yet possible to predict the residues important for the S100−target protein interaction.

S100B Has Two Equally Important TRTK-12 Binding Sites. Calcium binding to S100B results in the exposure of hydrophobic residues at its extreme C-terminus which have been implicated as important for interaction with target proteins in a calcium-dependent manner (*15, 42*). The truncation mutants S100B85stop and S100B83stop have several of these residues (A83, F87, F88) removed. Further, residue C84, shown by thiol accessibility experiments to become more exposed upon calcium binding, is also removed in the S100B83stop mutant (*43*). Compared to the native S100B protein, these mutants display 2000-fold weaker binding to TRTK-12, indicating the extreme C-terminus is an important component for protein binding. However, NMR experiments using the S100B85stop mutant identified significant chemical shift changes for residues S41, H42, and I47 of the linker region upon TRTK-12 binding. Since these

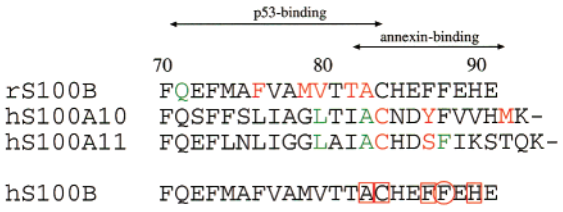

FIGURE 6: Key residues involved in S100−protein complexes. The C-terminal sequences of rat S100B, human S100A10, and human S100A11 are shown and numbered according to the S100B sequence. The buried surface area at each protein−peptide interface was calculated using the program VADAR (University of Alberta) based on three-dimensional structures for S100B−p53 (*35*), S100A10−annexin II (*33*), and S100A11−annexin I (*34*). Residues are color-coded depending on the extent of interaction with their corresponding target proteins; red = >50% decrease in side-chain surface area, green = 25−29% decrease in side-chain surface area upon peptide binding. Below is the C-terminal sequence for human S100B. Residue F88 where a significant decrease in TRTK-12 affinity was observed is circled while those residues that have significant chemical shift changes upon TRTK-12 binding are boxed.

changes occurred in the absence of the C-terminus of helix IV, a second site of interaction in the linker must exist. The relative energetic contributions of these two sites can be determined from the total binding energy of the TRTK-12 peptide for the full-length protein ($\Delta G_{binding} = -37.2$ kJ/mol) which must be the sum of the TRTK-12 binding contributions from the linker alone (ΔG_{linker}) and the C-terminus alone ($\Delta G_{C\text{-}terminus}$). The TRTK-12 affinity for S100B85stop ($\Delta G_{linker} = -17.9$ kJ/mol) corresponds to about 50% of the binding energy for the interaction of full-length S100B with TRTK-12, yielding $\Delta G_{C\text{-}terminus} = -19.3$ kJ/mol for the C-terminal residues H85−E91. Together these observations indicate that the energetic contributions of the linker and C-terminal regions are nearly equal for TRTK-12 binding. This finding is consistent with the sequence similarity of S100 proteins that shows the largest variations occur within these two regions (*11*, *44*, *45*). The energetic similarities of the linker and C-terminal regions in S100B would provide a convenient "dual" control for the recognition and binding of many proteins having little sequence similarity.

Comparison with Other S100 Target Protein Complexes. Using the TRTK-12 affinity results for the truncation mutant S100B85stop and the F8788A mutant, a comparison with other S100 protein complexes was done to establish whether the S100B−TRTK-12 complex bore any similarities to these existing structures. Three-dimensional structures of S100B, S100A10, and S100A11 in complex with fragments of the tumor suppressor protein p53, and the membrane proteins annexin II and annexin I, respectively, have recently been determined (*33*−*35*). The structures each show two distinct binding regions whereby the S100 protein recognizes its target substrate (Figure 6). In the S100B−p53 complex, the p53 peptide crosses helix IV and makes numerous contacts with helix III (*35*). In particular, the interaction site comprises approximately 240 Å^2 from side chains in helix IV of which Q71 and M79 supply roughly 50% of the contact surface area. The structures of the S100A11−annexin I and S100A10−annexin II complexes (*33*, *34*) also show two areas of interaction between the annexin peptides and their S100 partners. In these cases, the annexin peptides are oriented approximately 90° with respect to the p53 interaction, with S100B resulting in interactions more C-terminal along helix IV and including several contacts in the linker region of the S100 proteins. In helix IV, this results in major contacts between the annexin peptides and residues A81, C82, Y85, and M90 from S100A10 and residues A88, C89, and S92 from S100A11 (Figure 6). The surface areas of these interacting surfaces are very different, exhibiting about 147 Å^2 in S100A11 where C89 and F93 contribute >60% of the surface and 240 Å^2 in S100A10 where C82, Y85, and M90 contribute >80% of the surface.

In Figure 6, a summary is shown of the residues in helix IV from human S100B that have a significant decrease in TRTK-12 binding affinity and/or are affected in ^{1}H-^{15}N HSQC spectra monitoring TRTK-12 binding. The finding that residues 85−91 at the extreme C-terminus of S100B are important for TRTK-12 binding is most consistent with interactions observed in the three-dimensional structures of the S100A10−annexin II and S100A11−annexin I complexes. The significantly decreased affinity for TRTK-12 in the F88A and F8788A mutants shows that these residues contribute significantly to the target-binding site. These residues are analogous to Y85 and F86 in S100A10 and to S92 and F93 in S100A11. Further, the fluorescence results obtained here for F88A are nearly identical to studies of S100A10 where mutation of either Y85A or F86A shows decreased affinity for the annexin II peptide (*46*), consistent with the interactions of annexin II with Y86 observed in the three-dimensional structure (*33*). However, in S100B, it appears that both phenylalanine residues act together for interaction with TRTK-12 since the F87A mutation moderately increases TRTK-12 affinity. A similar increase in affinity was noted for a F86W mutant of S100A10, suggesting that F87 and F88 in S100B could provide a mechanism to finely tune the affinity for the broad spectrum of targets for S100 proteins. This hypothesis is supported by sequence analysis of the C-termini of S100 proteins that exhibit conservation of a bulky hydrophobic residue (F, M, I, L) at position 88 and a broad variability at position 87 (A, F, Y, S, N, K).

The S100B85stop mutant showed a binding energy approximately 50% of that for the full-length protein. Again, this observation is nearly identical to S100A10 where annexin II binding was undetectable when residues C-terminal to, and including Y86, were deleted (*46*). Analysis of the three-dimensional structures of Ca^{2+}-S100B shows that all of the residues beyond C84 (i.e., the deleted residues) have greater than 50% of their side chains exposed to solvent. However, the interaction of TRTK-12 with S100B shows little sensitivity to pH or ionic strength, suggesting that salt bridge interactions involving E86, E89, and E91 are likely not significant. Further, the pK_a values of the two histidine residues in this region, H85 (6.70) and H90 (7.13), are near that expected for an exposed histidine, suggesting H85 and H90 are not buried at the protein−peptide interface. Aside from the decreased affinity resulting from mutation of F8788A, there must be other factors in this region that affect TRTK-12 affinity. From our structural comparison of S100B85stop with full-length S100B, both in the presence of TRTK-12, it is apparent that the extreme C-terminus of the S100B85stop protein is unstructured as opposed to α-helical as observed in the wild-type protein. Since binding is drastically reduced in S100B85stop, this would provide

evidence for residues near this region, including A83 and C84, to be involved in interactions with TRTK-12. This would be consistent with observations that the analogous residues in S100A10 and S100A11 are involved in interactions with their annexin partners (Figure 6). Further, A83 is among the residues most affected by TRTK-12 binding as monitored by NMR spectroscopy.

While the proposed interaction of TRTK-12 with the C-terminus of S100B appears similar to protein interactions for S100A10 and S100A11, there are obviously some important differences. For example, the TRTK-12 sequence bears little similarity to sequences for the annexin I and II peptides and is only remotely similar to the p53 sequence. Further, the protein sequences near the C-terminus are highly variable (Figure 6), as has been noted for the S100 family in general (*11*, *44*, *45*), although it is interesting that S100B, S100A10, and S100A11 all have a common ACxxxF motif. Finally, even the S100A10 and S100A11 interactions with annexins I and II are variable based on different surface areas and some of the residues involved, so it might be expected that the TRTK-12 interaction will have modified interactions within the peptide sequence and the C-terminus of S100B compared to either S100A10 or S100A11. Understanding these interactions will be a key to determining the specificity of each S100 protein for its range of target proteins.

ACKNOWLEDGMENT

We thank Kathy Barber for excellent technical assistance and maintenance of the NMR spectrometer. We also thank Abbie Grigg for sedimentation equilibrium data on S100B83stop and S100B85stop and Dr. S. J. Dixon (Department of Physiology, University of Western Ontario) for the use of his fluorescence spectrophotometer. In addition, we thank Robert Boyko and Dr. Brian Sykes for providing the Xcrvfit and VADAR programs.

REFERENCES

1. Finn, B. E., Evenas, J., Drakenberg, T., Walthro, J. P., Thulin, E., and Forsen, S. (1995) *Nat. Struct. Biol. 2*, 777−783.
2. Gagne, S. M., Tsuda, S., Li, M. X., Smillie, L. B., and Sykes, B. D. (1995) *Nat. Struct. Biol. 2*, 784−789.
3. Kuboniwa, H., Tjandra, N., Grzesiek, S., Ren, H., Klee, C. B., and Bax, A. (1995) *Nat. Struct. Biol. 2*, 768−776.
4. Zhang, M., Tanaka, T., and Ikura, M. (1995) *Nat. Struct. Biol. 2*, 758−767.
5. Kretsinger, R. H., Rudnick, S. E., and Weissman, L. J. (1986) *J. Inorg. Biochem. 28*, 289−302.
6. Babu, Y. S., Bugg, C. E., and Cook, W. J. (1988) *J. Mol. Biol. 203*, 191−204.
7. Herzberg, O., and James, M. N. G. (1988) *J. Mol. Biol. 203*, 761−779.
8. Satyshur, K. A., Rao, S. T., Pyzalska, D., Drendel, W., Greaser, M., and Sundaralingam, M. (1988) *J. Biol. Chem. 263*, 1628−1647.
9. Satyshur, K. A., Pyzalska, D., Greaser, M., Rao, S. T., and Sundaralingam, M. (1994) *Acta Crystallogr. D 50*, 40−49.
10. Slupsky, C. M., Kay, C. M., Reinach, F. C., Smillie, L. B., and Sykes, B. D. (1995) *Biochemistry 34*, 7365−7375.
11. Potts, B. C. M., Smith, J., Akke, M., Macke, T. J., Okazaki, K., Hidaka, H., Case, D. A., and Chazin, W. J. (1995) *Nat. Struct. Biol. 2*, 790−796.
12. Drohat, A. C., Amburgey, J. C., Abildgaard, F., Starich, M. R., Baldisseri, D., and Weber, D. J. (1996) *Biochemistry 35*, 11577−11588.
13. Kilby, P. M., Van Eldik, L. J., and Roberts, G. C. K. (1996) *Structure 4*, 1041−1052.
14. Drohat, A. C., Baldisseri, D. M., Rustandi, R. R., and Weber, D. J. (1998) *Biochemistry 37*, 2729−2740.
15. Smith, S. P., and Shaw, G. S. (1998) *Structure 6*, 211−222.
16. Matsumura, H., Shiba, T., Inoue, T., Harada, S., and Kai, Y. (1998) *Structure 6*, 233−241.
17. Smith, S. P., and Shaw, G. S. (1998) *Biochem. Cell Biol. 76*, 324−333.
18. Donato, R. (1999) *Biochim. Biophys. Acta 1450*, 191−231.
19. Smith, S. P., and Shaw, G. S. (1997) *J. Biomol. NMR 10*, 77−88.
20. Baudier, J., Mochly-Rosen, D., Newton, A., Lee, S.-H., Koshland, D. E., and Cole, R. D. (1987) *Biochemistry 26*, 2886−2893.
21. Baudier, J., and Cole, R. D. (1988) *J. Biol. Chem. 263*, 5876−5883.
22. Sheu, F.-S., Huang, F. L., and Huang, K.-P. (1995) *Arch. Biochem. Biophys. 316*, 335−342.
23. Lin, L.-H., Van Eldik, L. J., Osheroff, N., and Norden, J. J. (1994) *Mol. Brain Res. 25*, 297−304.
24. Garbuglia, M., Verzini, M., Giambanco, I., Spreca, A., and Donato, R. (1996) *FASEB J. 10*, 317−324.
25. Bianchi, R., Giambanco, I., and Donato, R. (1993) *J. Biol. Chem. 268*, 12669−12674.
26. Donato, R. (1988) *J. Biol. Chem. 263*, 106−110.
27. Bianchi, R., Garbuglia, M., Verzini, M., Giambanco, I., Ivanenkov, V. V., Dimlich, R. V. W., Jamieson, G. A., Jr., and Donato, R. (1996) *Biochim. Biophys. Acta 1313*, 258−267.
28. Ivanenkov, V. V., Jamieson, G. A., Jr., Gruenstein, E., and Dimlich, R. V. W. (1995) *J. Biol. Chem. 270*, 14651−14658.
29. McClintock, K. A., and Shaw, G. S. (2000) *Protein Sci. 9*, 2043−2046.
30. Barber, K. R., McClintock, K. A., Jamieson, G. A., Jr., Dimlich, R. V., and Shaw, G. S. (1999) *J. Biol. Chem. 274*, 1502−1508.
31. McKay, R. T., Tripet, B. P., Hodges, R. S., and Sykes, B. D. (1997) *J. Biol. Chem. 272*, 28494−28500.
32. Zhan, Q., Wong, S. S., and Wang, C. L. A. (1991) *J. Biol. Chem. 266*, 21810−21814.
33. Rety, S., Sopkova, J., Renouard, M., Osterloh, D., Gerke, V., Tabaries, S., Russo-Marie, F., and Lewit-Bentley, A. (1999) *Nat. Struct. Biol. 6*, 89−95.
34. Rety, S., Osterloh, D., Arie, J.-P., Tabaries, S., Seeman, J., Russo-Marie, F., Gerke, V., and Lewit-Bentley, A. (2000) *Structure 8*, 175−184.
35. Rustandi, R. R., Baldisseri, D. M., and Weber, D. J. (2000) *Nat. Struct. Biol. 7*, 570−574.
36. Smith, S. P., Barber, K. R., Dunn, S. D., and Shaw, G. S. (1996) *Biochemistry 35*, 8805−8814.
37. Van Eldik, L. J., Staecker, J. L., and Winningham-Major, F. (1988) *J. Biol. Chem. 263*, 7830−7837.
38. Kay, L. E., Keifer, P., and Saarinen, T. (1992) *J. Am. Chem. Soc. 114*, 10663−10665.
39. Shuker, S. B., Hajduk, P. L., Meadows, R. P., and Fesik, S. W. (1996) *Science 274*, 1531−1534.
40. Shaw, G. S., Golden, L. F., Hodges, R. S., and Sykes, B. D. (1991) *J. Am. Chem. Soc. 113*, 5557−5563.
41. Shoemaker, K. R., Kim, P. S., York, E. J., Stewart, J. M., and Baldwin, R. L. (1987) *Nature 326*, 563−567.
42. Heizmann, C. W., and Cox, J. A. (1998) *Biometals 11*, 383−397.
43. Petrova, T. V., Hu, J., and Van Eldik, L. J. (2000) *Brain Res. 853*, 74−80.
44. Schafer, B. W., and Heizmann, C. W. (1996) *Trends Biochem. Sci. 21*, 134−140.
45. Heizmann, C. W., and Hunziker, W. (1991) *Trends Biochem. Sci. 16*, 98−103.
46. Kube, E., Becker, T., Weber, K., and Gerke, V. (1992) *J. Biol. Chem. 267*, 14175−14182.

BI011732M